Mechanical and electronic properties of CeO_2, ThO_2, and $(Ce,Th)O_2$ alloys

C. Sevik* and T. Çağın†
Department of Chemical Engineering & Material Science and Engineering, Texas A&M University, College Station, Texas 77845-3122, USA

(Received 30 April 2009; revised manuscript received 25 June 2009; published 17 July 2009)

A systematic first-principle study is conducted to calculate bulk modulus, elastic constants, phonon-dispersion curves, and electronic structures of CeO_2, ThO_2, and their ordered binary alloys $Ce_xTh_{8-x}O_{16}$ with $x=1$, 2, 4, 6, and 7 using local-density approximation (LDA), generalized gradient approximation (GGA), LDA+U, and GGA+U approaches. In order to get accurate results for these type of systems including f electrons [Ce($4f$) and Th($5f$)] we optimized the U parameter for use in LDA+U and GGA+U approaches. The computed structural, mechanical, and electronic properties of CeO_2 and ThO_2 are observed to display strong correlation with experimental data. In particular, the best agreement with experiment is obtained within the LDA+U in which on-site Coulomb interaction parameter (U_{eff}) for Ce and Th are taken as 6.0 and 5.0 eV. To check the stability of alloy forms, phonon-dispersion curves of $Ce_xTh_{8-x}O_{16}$ with $x=2$, 4, and 6 are computed. In all concentrations, mechanical stability conditions are satisfied for alloys. Furthermore, we observed no negative phonon branches in the phonon spectrum of alloys. Our calculations indicated a strong effect of concentration, x, on the electronic structure of $Ce_xTh_{8-x}O_{16}$.

DOI: 10.1103/PhysRevB.80.014108 PACS number(s): 62.20.D−, 21.60.De, 61.66.Dk

I. INTRODUCTION

The rare-earth oxide CeO_2 (ceria) and actinide-oxide ThO_2 (thoria) are very important materials for technological and industrial applications. For instance, CeO_2 is widely used in catalysis and fuel cell applications due to its ability to take and release oxygen under oxidizing and reducing conditions.[1,2] Two particular physical properties of fluorite type CeO_2, the lattice mismatch to Si and high dielectric constant, make ceria a potential material for use in microelectronic applications, high-quality epitaxy on Si[3] and buffer layers of high-temperature superconductors.[4] Among several applications of ThO_2, the most important one is its potential use in nuclear energy applications. Specifically, the ThO_2 matrix with admixture of uranium and plutonium oxides is used as advanced fuel materials for nuclear reactors.[5] Plutonium is emulated by cerium in many laboratory experiments on the $(Th,Pu)O_2$ due to the inconvenience resulting from its high radioactivity and scarcity. Consequently, a thorough understanding of the structural and electronic properties of $(Ce,Th)O_2$ alloys is crucial for efficient processing of admixture type in new generation nuclear fuels.[6]

On account of this obvious importance, several studies have already been conducted for both of these compounds. Brillouin-zone-center phonon frequencies,[7–11] phonon-dispersion curves along high-symmetry lines,[12] and elastic constants of these two important oxides[13–15] have been measured by several methods. The variety of experimental results reported on the bulk modulus of ThO_2 (Refs. 12 and 15–18) with values ranging between 193 and 262 GPa still provokes discussions. The high-pressure α-$PbCl_4$-type phase of the two compounds have also been investigated and the transition pressures have been reported as 31 GPa for CeO_2 (Refs. 13 and 19) and 36 GPa for ThO_2.[18]

On the theoretical side, a small number of calculations have been published for ThO_2 (Refs. 20–25) in contrast to the number of studies related with CeO_2. Particularly, *ab initio* phonon-dispersion curves of ThO_2 have not been considered yet with an accurate approximation. As for CeO_2, numerous calculations are available and are carried out by several methods such as periodic Hartree-Fock,[26] self-interaction-corrected local-spin-density approximation,[27,28] local-density approximation (LDA), and generalized gradient approximation (GGA) within the density-functional theory (DFT).[1,28–37] On the other hand, there are only a limited number of first-principles studies on the lattice dynamics of these two compounds.

The debate on the methods to investigate systems with localized (strongly correlated) f electrons still continues in the literature. Many researchers believe that conventional DFT techniques based on LDA or GGA would be unable to cope with these systems. This belief is supported by the current literature on ceria.[1,26,35,36,38] Meanwhile, Gürel *et al.*[39] have performed *ab initio* calculations for CeO_2 by treating $4f$ electrons as valance electrons and their results on the phonon-dispersion curves, mode-Grüneisen parameters, dielectric permittivity tensor, and Born effective charges have shown good agreement with the available experimental data. The well-established DFT+U approach[40] is applied to studies on CeO_2.[31,34,36,37,41] Within this method Hartree-Fock type interactions are parameterized with Coulomb (U) and exchange (J) terms.

In this work, we have focused on accurate determination of structural and electronic properties of CeO_2, ThO_2, and their alloys by using DFT. All calculations have been performed with and without the Hubbard-type on-site Coulomb interaction (+U approach) in order to understand the overall effect of f electrons on physical properties of these pure compounds and their alloys. The important feature of this work, unlike commonly studied pure bulk systems, is that we have consider five different concentration of alloys: $CeTh_7O_{16}$, Ce_7ThO_{16}, $Ce_2Th_6O_{16}$, $Ce_6Th_2O_{16}$, and $Ce_4Th_4O_{16}$. Phonon-dispersion curves at each concentration have been determined by using the frozen phonon approxi-

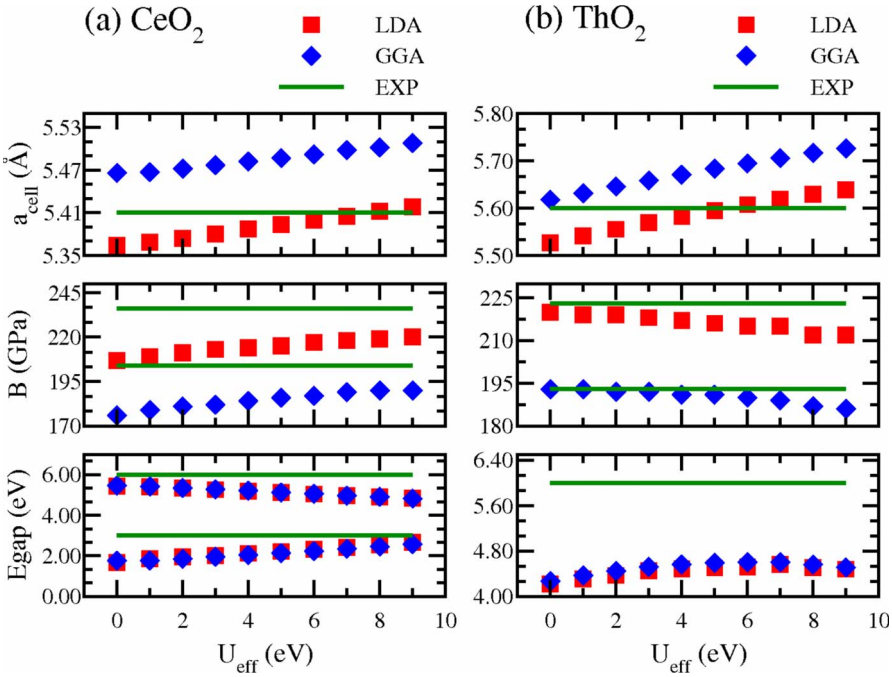

FIG. 1. (Color online) For CeO_2 and ThO_2, variation in equilibrium lattice constant, bulk modulus, and energy gap with U_{eff}. Red squares and blue diamonds show LDA and LDA+U type calculations, and green lines shows experimental data.

mation, the ionic forces obtained by DFT, to check the stability of the alloys of these compounds.

II. COMPUTATIONAL APPROACHES

Structural, electronic, and vibrational properties of CeO_2, ThO_2, and their ordered alloys have been calculated within the density-functional theory,[42] using the projector augmented wave pseudopotential formalism[43,44] as implemented in Vienna *ab initio* simulation package (VASP).[45,46] The electronic exchange and correlation functions have been treated by utilizing both LDA and Perdew-Burke-Ernzerhof[47] form of GGA together with their on-site Coulomb interaction added versions, (LDA+U) and (GGA+U).[40] In the case of the DFT+U calculations Hubbard-type on-site Coulomb interaction has been considered by employing a rotationally invariant method proposed by Dudarev *et al.*[48] in which the total energy just depends on the difference between the Coulomb, U, and exchange, J, parameters. In order to determine the $U_{eff}=U-J$ for each material, available experimental data such as lattice constant (a_0), bulk modulus (B_0), and electronic band gap (E_{gap}) have been compared with the calculated values. Hence, U_{eff} is treated as an empirical fitting parameter. For all calculations 650 eV plane-wave energy cutoff and minimum $4\times4\times4$ Monckhorst-Pack k point grid

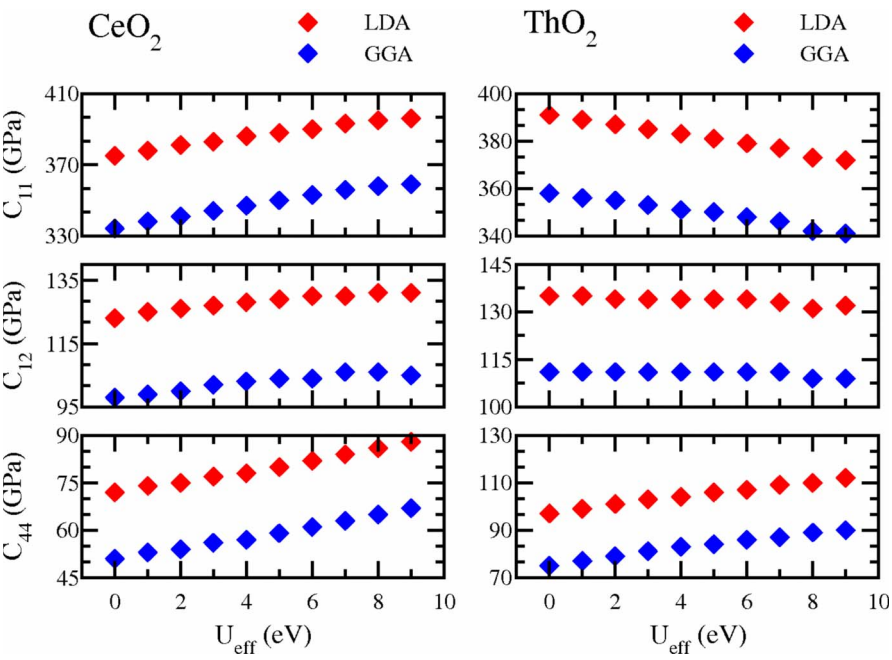

FIG. 2. (Color online) The variation in elastic constants C_{11}, C_{12}, and C_{44} with U_{eff} for (a) CeO_2 and (b) ThO_2.

TABLE I. For CeO_2 and ThO_2, comparison of structural and electronic properties calculated with both LDA and LDA+U (U_{eff}=6.0 eV for CeO_2 and U_{eff}=5.0 eV for ThO_2) to other theoretical and experimental results. PW=present work.

CeO_2	a_0	B_0	C_{11}	C_{12}	C_{44}	E_g	Ref.
LDA+U, 6 eV	5.40	217	390	130	82	5.04	PW
LDA	5.36	207	375	123	72	5.43	PW
LDA	5.37	210	386	124	73		39
Expt.			450	117	57		12
Expt.			403	105	60		14
LDA+U, 5 eV	5.40	214				5.00	36
LDA+U, 5.3 eV	5.40	210				5.61	37
LDA	5.38	211				5.60	31
LDA	5.39	215				5.50	1
LDA	5.33	218					20
Expt.	5.41	204–236				6.00	Ref.[a]
ThO_2	a_0	B_0	C_{11}	C_{12}	C_{44}	E_g	
LDA+U, 5 eV	5.60	216	381	134	106	4.50	PW
LDA	5.30	220	391	135	97	4.22	PW
Expt.			377	146	89		12
Expt.			367	106	79		14
GGA-92	5.61	189	355	106	54	4.82	24
LDA	5.52	225					20
LDA	5.52	225					16
GGA	5.61	198					16
Expt.	5.60	193–262				6.0	Ref.[b]

[a]References 12, 13, 19, and 28.
[b]References 12, 15–18, and 25.

have been used to limit the total-energy convergence to less than 3 meV.

Bulk modulus and its pressure derivative for each material have been determined by fitting the calculated equation of state (EOS) data to the third-order Vinet EOSs.[49] In the Vinet EOS, the total energy as a function of volume is given as

$$E = E_0 + \frac{4B_0V_0}{(B_0'-1.0)^2} - \frac{2V_0B_0}{(B_0'-1)^2}[5+3B_0'(x-1)-3x] \times \exp\left[-\frac{3}{2}(B_0'-1)(x-1)\right], \quad (1)$$

where E_0 is the total energy, V_0 is the equilibrium volume, B_0 is the bulk modulus at $P=0$ GPa, B_0' is the first derivative of the bulk modulus with respect to pressure, and $x=(V/V_0)^{1/3}$. The elastic constants of each structure have also been obtained by using the same procedure followed by Cagin and co-workers.[50]

Phonon-dispersion relations for each structure have been determined by using *ab initio* force-constant method as described in Parlinski *et al.*[51] In order to correct LO-TO splitting for CeO_2 and ThO_2, Born effective charges have been calculated with the finite difference method as implemented in VASP code.[52]

III. RESULTS

A. Pure crystals

The paramagnetic phase of $CeO_2(ThO_2)$ has conventional cubic $Fm\bar{3}m$ CaO_2 (fluorite) structure with three atoms per primitive fcc cubic cell; one Ce(Th) and two O atoms are located at reduced positions (0,0,0) and $\pm(1/4,1/4,1/4)$, respectively. First, to determine the U_{eff} parameter for these two oxides a_0 and B_0, and band gap [E_{gap}^{2p-4f}=O($2p$)-Ce($4f$) and E_{gap}^{2p-5d}=O($2p$)-Ce($5d$) for CeO_2 and E_{gap}=O($2p$)-Th($6d$) for ThO_2] values are calculated by both LDA+U and GGA+U, and then these results are compared with the experimental data as shown in Fig. 1. Eventually, it is predicted that the inclusion of Hubbard-type on-site electron interaction in either LDA or GGA changes the results marginally for both materials. However, our a_0 and B_0 values calculated by the LDA+U approach with U_{eff} values 6 eV (consistent with the literature[31,36,37,53]) for CeO_2 and 5 eV for ThO_2 compare well with the experimental data as listed in Table I. In addition to consistent reproduction of a_0 and B_0 with the chosen values of U_{eff} for both structures, the calculated values for band gaps are reasonably good, given the well-known fact that DFT underestimate band gaps of insulators and semiconductors by 30% and 40%. Furthermore, our systematic study of these three parameters shows that the

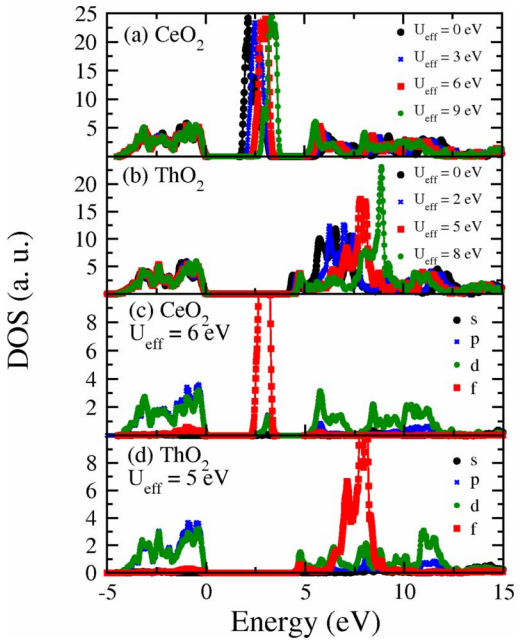

FIG. 3. (Color online) Total DOS calculated with various U_{eff} values for (a) CeO_2 and (b) ThO_2. Angular momentum-resolved DOS calculated with (c) U_{eff}=6.0 eV for CeO_2 and (d) U_{eff} =5.0 eV for ThO_2.

LDA+U approach works better than GGA+U for both of these crystals as indicated in the CeO_2 study of some other groups.[36,37,54]

Three independent elastic constants of CeO_2 and ThO_2 are calculated by using both LDA and LDA+U approaches. These 0 K temperature elastic constants agree quite well with the available experimental ones as given in Table I. Additionally, the results clearly show that the effect of the Hubbard term is insignificant for the mechanical properties and supports the findings of earlier reports along this line (see Fig. 2).

The total density of states (DOS) (Fig. 3), angular momentum-resolved DOS (Fig. 3), and band structure (Fig. 4) of these two systems are determined with and without set U_{eff} values within the LDA approach. A common trend can be proposed from total DOS graphs: the influence of U_{eff} on the electronic structure is basically restricted to the empty f band and this does not drastically change the band structures

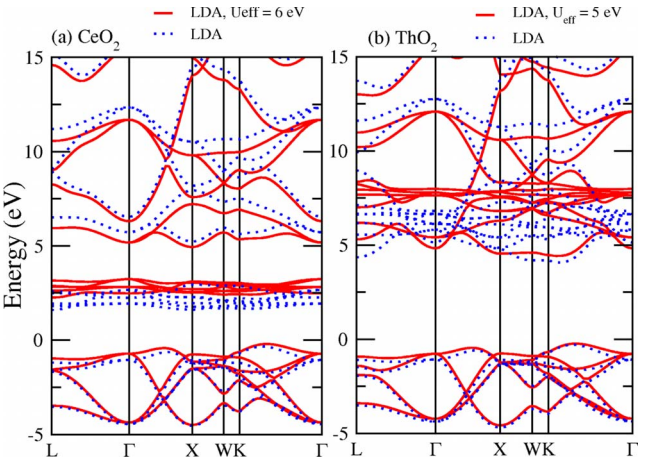

FIG. 4. (Color online) Electronic band structure for (a) CeO_2 and (b) ThO_2. The red continuous lines show LDA+U results calculated with U_{eff}=6.0 eV for CeO_2 and U_{eff}=5.0 eV for ThO_2, and blue dotted lines show LDA results.

especially occupied states as shown in Fig. 4. Additionally, inspecting the same figure, we conclude that the effective masses at the high-symmetry points for the states out of f remain identical. The main difference between the electronic structure of these two oxides is that these vacant f states (most influenced) lie above the Th(6d) state in ThO_2 while appearing in the gap between the O(2p) and Ce(5d) states in CeO_2. For CeO_2, the width of the 2P band calculated with the set U_{eff} is about 4 eV and is within the experimental error.[55–57] Moreover, our LDA results obtained with a defined U_{eff} value show the usual underestimation of the band gap within the standard DFT. Hence, the band gaps [O(2p)-Ce(4f) E_{gap}=2.21 eV and O(2p)-Ce(5d) E_{gap} =5.12 eV for CeO_2 and O2p-Ce(6d) E_{gap}=4.52 eV for ThO_2] are slightly smaller than the measured ones, 3.00, 6.00,[36] and 5.75 eV;[25] thus they are all acceptable.

The phonon-dispersion relations are obtained with the frozen phonon technique in order to better understand the overall effect of the +U approach and to check the validity of our defined U_{eff} values. As seen in Fig. 5, the two phonon-dispersion curves along the $\Gamma-X-K-\Gamma-X-W-L$ directions obtained with and without the +U approach are quite similar. Therefore the +U approach has marginal effect on phonon dispersions of the two compounds as in the structural prop-

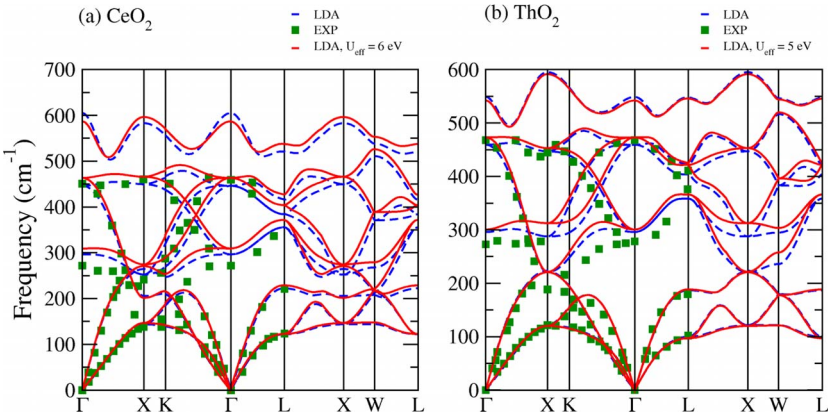

FIG. 5. (Color online) Phonon-dispersion relations of the (a) CeO_2 and (b) ThO_2. The red continuous lines show LDA+U results calculated with U_{eff} =6.0 eV for CeO_2 and U_{eff} =5.0 eV for ThO_2, blue dashed lines show LDA results, and green squares show experimental data (Ref. 12).

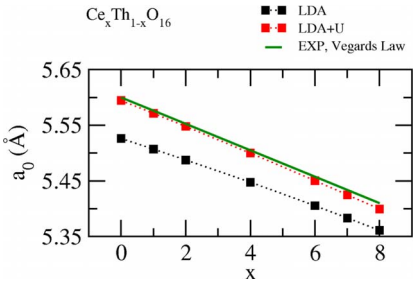

FIG. 6. (Color online) The variation in equilibrium lattice constants of $Ce_xTh_{8-x}O_{16}$ with respect to x, calculated with both LDA and LDA+U, U_{eff}=6.0 for Ce and U_{eff}=5.0 for Th.

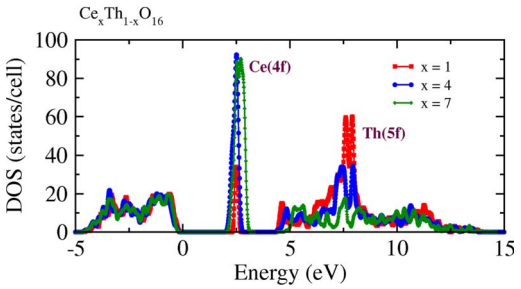

FIG. 7. (Color online) Calculated LDA+U total DOS of $Ce_xTh_{8-x}O_{16}$ for x=1, 4, and 7. U_{eff}=6.0 for Ce and U_{eff}=5.0 for Th.

erties. The usual over estimation of T_{2u} TO mode, commented by Gürel *et al.*[39] to be a known problem of fluorite structures, is observed once more for both CeO_2 and ThO_2. Overall, the general agreement between our results and the experimental data are excellent. Born effective charges of Ce and O for CeO_2 and Th and O for ThO_2 are found to be $Z^{\star}_{Ce}$=5.782, $Z^{\star}_{O}$=2.891, $Z^{\star}_{Th}$=5.356, and $Z^{\star}_{O}$=2.678 with LDA and $Z^{\star}_{Ce}$=5.519, $Z^{\star}_{O}$=2.760, $Z^{\star}_{Th}$=5.327, and $Z^{\star}_{O}$=2.663 with LDA+U. The calculated effective charges of CeO_2 are in close agreement with previous theoretical studies.[33,39] Finally, the insignificant effect of the +U approach could be seen not only on structural parameters but also on calculated Born effective charges which are critical to predict the LO-TO splitting.

B. Alloying

As the key objective of our work, we carried out calculations to predict physical properties of binary ordered CeO_2-ThO_2 alloys as a function of concentration. Despite the fact that we have shown the marginal influence of the +U approach on CeO_2 and ThO_2 crystals, we have selected the U_{eff} values providing general agreement with the experiment, 6 eV for Ce and 5 eV for Th in LDA+U calculations of alloy compounds. Using $Ce_xTh_{8-x}O_{16}$ as the generic notation, five different concentration of alloy forms, $CeTh_7O_{16}$ and Ce_7ThO_{16} with symmetry $Fm\bar{3}m$, $Ce_2Th_6O_{16}$ and $Ce_6Th_2O_{16}$ with symmetry $Pm\bar{3}m$, and $Ce_4Th_4O_{16}$ with symmetry $P4/mmm$ are handled. Relaxed equilibrium lattice constants vs concentration results obtained by LDA and LDA+U closely follow Vegard's law represented by the straight line in Fig. 6. The calculated bulk modulus and elastic constants for alloys are listed in Table II as well. The similarity between B_0 and elastic constants values for different alloy concentrations is not surprising because the two crystals have comparable structural and mechanical properties. Calculated elastic constants also follow the Vegard's law; this behavior can be clearly seen from the C_{44} and $(C_{11}$-$C_{12})/2$ values listed in Table II, which is obtained directly from tetragonal shear and pure shear application to the unit cells. The deviation from Vegard's law is mainly due to the bulk modulus, $B_0=(C_{11}+2C_{12})/3$, obtained from Vinet EOS fitting, then used for solving individual elastic constants.

Calculated DOS of $Ce_xTh_{8-x}O_{16}$ with x=1, 4, and 7 are represented in Fig. 7. The interesting finding obtained from this figure is that the density of f state located at the intermediate zone of band gap and just above the d state [labeled as Ce(4f) and Th(5f) in figure] strongly depend on x. This is because as the location of the f state in the energy axis for the CeO_2 (within the band gap) and ThO_2 (after the gap) (cf. Fig. 3). This feature may allow us to manipulate f-state concentration between the band gap of alloys by varying concentration in the mixture. As a final result of the electronic structure calculations, we can call attention to the fact that

TABLE II. Calculated lattice parameters, mechanical properties, and band-gap values for $Ce_xTh_{1-x}O_{16}$. Two E_{gap} corresponds to energy gaps between p-Ce(4f) and p-Th(5f) states, see Fig. 7.

	a_0	B_0	C_{11}	C_{12}	C_{44}	E_{gap}	Alloy
LSDA+U	5.571	214	379	131	104	2.254.28	$Ce_1Th_7O_{16}$
LDA	5.507	216	386	131	95	1.664.09	
LSDA+U	5.548	215	382	132	101	2.124.15	$Ce_2Th_6O_{16}$
LDA	5.488	215	385	130	92	1.534.11	
LSDA+U	5.500	213	382	129	96	1.924.19	$Ce_4Th_4O_{16}$
LDA	5.448	210	379	126	87	1.354.16	
LSDA+U	5.450	215	386	130	88	1.884.34	$Ce_6Th_2O_{16}$
LDA	5.405	209	377	125	79	1.344.70	
LSDA+U	5.425	216	388	130	85	1.984.55	$Ce_7Th_1O_{16}$
LDA	5.383	208	376	124	76	1.495.00	

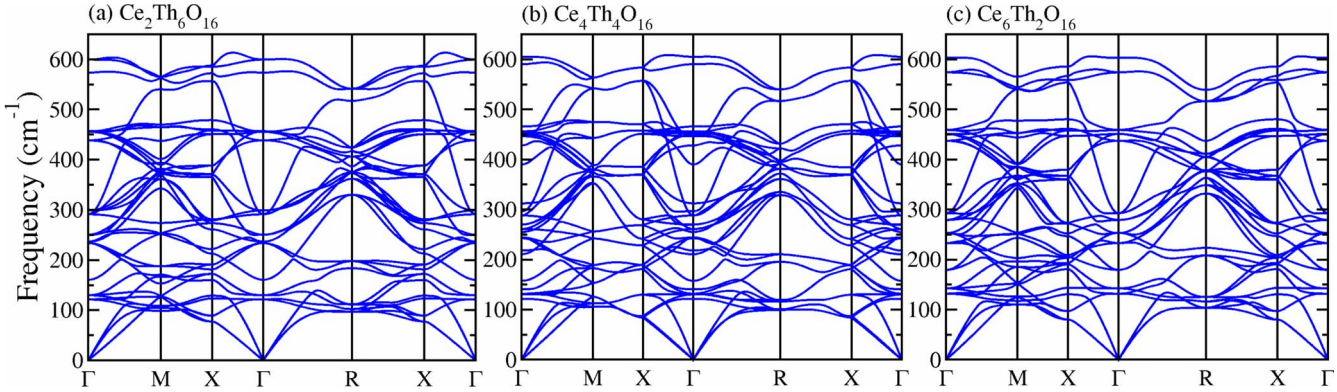

FIG. 8. (Color online) Calculated LDA Phonon dispersion of $Ce_xTh_{1-x}O_{16}$ with $x=2$, 4, and 6.

$p-f$ and $p-d$ band-gap values are marginally different from each other as seen in Table II.

An important concern is the thermomechanical stability of these alloy structures. Calculated elastic constants with both LDA and LDA+U approaches satisfy the mechanical stability conditions of cubic crystals; $(C_{11}-C_{12})>0$, $C_{44}>0$, and $C_{11}+2C_{12}>0$ (cf. Table II). For the rest, we compute the phonon-dispersion curves of $Ce_xTh_{8-x}O_{16}$ with $x=2$, 4, and 6 with force obtained by LDA. It can be inferred from Fig. 8 that all of these alloy formations are at least locally stable. Because of the computational restrictions, phonon-dispersions curves of $Ce_xTh_{8-x}O_{16}$ with $x=1$ and 7 could not been computed. However, the mechanical stability conditions satisfied by the calculated elastic constants and bulk modulus of these alloys are satisfactory for the stability of these two phases.

IV. CONCLUSIONS

To summarize, we perform systematic first-principles calculations to obtain structural and electronic properties of alloy formations of CeO_2 and ThO_2. To achieve our goal, first we realize a set of simulations to predict Coulomb U and exchange J parameters for both CeO_2 and ThO_2 used in LDA+U and GGA+U approaches. The LDA+U method gives better agreement than the GGA+U method, and the most convenient results are obtained by $U_{eff}=6.0$ eV and $U_{eff}=5.0$ eV for Ce and Th, respectively. All the same, the marginal effect of U_{eff} is stated for both of these paramagnetic oxides. Consequently, structural and electronic properties of $C_xTh_{8-x}O_{16}$ with $x=1$, 2, 4, 6, and 7 are predicted with reasonable accuracy. Additionally, it is observed that the electronic structure of these alloys show interesting behavior because of the f electrons of the CeO_2 and ThO_2.

ACKNOWLEDGMENT

The work performed is partially supported by LLNS/INSER program.

*sevik@neo.tamu.edu
†tcagin@tamu.edu

[1] N. V. Skorodumova, R. Ahuja, S. I. Simak, I. A. Abrikosov, B. Johansson, and B. I. Lundqvist, Phys. Rev. B **64**, 115108 (2001).
[2] M. S. Dresselhaus and I. L. Thomas, Nature (London) **414**, 332 (2001).
[3] T. Inoue, Y. Yamamoto, S. Koyama, S. Suzuki, and Y. Ueda, Appl. Phys. Lett. **56**, 1332 (1990).
[4] L. Luo, X. D. Wu, R. C. Dye, R. E. Muenchausen, S. R. Foltyn, Y. Coulter, C. J. Maggiore, and T. Inoue, Appl. Phys. Lett. **59**, 2043 (1991).
[5] I. R. Shein, K. I. Shein, and A. L. Ivanovskii, J. Nucl. Mater. **361**, 69 (2007).
[6] Y. Altaş and H. Tel, J. Nucl. Mater. **298**, 316 (2001).
[7] N. I. Santha, M. T. Sebastian, P. Mohanan, N. M. Alford, R. C. Sarma, K. Pullar, S. Kamba, A. Pashkin, P. Samukhina, and J. Petzelt, J. Am. Ceram. Soc. **87**, 1233 (2004).
[8] W. H. Weber, K. C. Hass, and J. R. McBride, Phys. Rev. B **48**, 178 (1993).
[9] S. Kanakaraju, A. K. Mohan, and S. Sood, Thin Solid Films **305**, 191 (1997).
[10] S. Wang, J. Wang, W. Zuo, and Y. Qian, Mater. Chem. Phys. **68**, 246 (2001).
[11] I. Kosacki, T. Suzuki, H. U. Anderson, and P. Colomban, Solid State Ionics **149**, 99 (2002).
[12] K. Clausen, W. Hayes, E. J. Macdonald, R. Osborn, and G. P. Schnabel, J. Chem. Soc., Faraday Trans. 2 **83**, 1109 (1987).
[13] L. Gerward and J. Staun Olsen, Powder Diffr. **8**, 127 (1983).
[14] A. Nakajima, A. Yoshihara, and M. Ishigame, Phys. Rev. B **50**, 13297 (1994).
[15] P. M. Macedo, W. Capps, and J. B. Watchman, J. Am. Ceram. Soc. **47**, 651 (1964).
[16] S. J. Olsen, L. Gerward, V. Kanchana, and G. Vaitheeswaran, J. Alloys Compd. **381**, 37 (2004).
[17] J. P. Dancausse, E. Gering, S. Heathman, and U. Benedict, High Press. Res. **2**, 381 (1990).
[18] M. Idiri, T. Le Bihan, S. Heathman, and J. Rebizant, Phys. Rev. B **70**, 014113 (2004).
[19] S. J. Duclos, Y. K. Vohra, A. L. Ruoff, A. Jayaraman, and G. P.

Espinosa, Phys. Rev. B **38**, 7755 (1988).
[20] V. Kanchana, G. Vaitheeswaran, A. Svane, and A. Delin, J. Phys.: Condens. Matter **18**, 9615 (2006).
[21] J. P. Kelly and M. S. S. Brooks, J. Chem. Soc., Faraday Trans. 2 **83**, 1189 (1987).
[22] J. H. Harding, P. J. D. Lindan, and N. C. Pyper, J. Phys.: Condens. Matter **6**, 6485 (1994).
[23] S. Li, R. Ahuja, and B. Johansson, High Press. Res. **22**, 471 (2002).
[24] R. Terki, G. Feraoun, H. Bertrand, and H. Aourag, Comput. Mater. Sci. **33**, 44 (2005).
[25] E. T. Rodine and P. L. Land, Phys. Rev. B **4**, 2701 (1971).
[26] S. Gennard, F. Corà, and C. R. A. Catlow, J. Phys. Chem. B **103**, 10158 (1999).
[27] L. Petit, A. Svane, Z. Szotek, and W. M. Temmerman, Phys. Rev. B **72**, 205118 (2005).
[28] L. Gerward, S. J. Olsen, V. Kanchana, G. Vaitheeswaran, and A. Svane, J. Alloys Compd. **400**, 56 (2005).
[29] G. A. Landrum, R. Dronskowski, R. Niewa, and F. J. DiSalvo, Chem.-Eur. J. **5**, 515 (1999).
[30] D. D. Koelling, A. M. Boring, and J. H. Wood, Solid State Commun. **47**, 227 (1983).
[31] S. Fabris, S. de Gironcoli, S. Baroni, G. Vicario, and G. Balducci, Phys. Rev. B **71**, 041102(R) (2005).
[32] C. J. Pickard, B. Winkler, R. K. Chen, M. C. Payne, M. H. Lee, J. S. Lin, J. A. White, V. Milman, and D. Vanderbilt, Phys. Rev. Lett. **85**, 5122 (2000).
[33] T. Yamamoto, T. Uda, T. Hamada, H. Momida, and T. Ohno, Thin Solid Films **486**, 136 (2005).
[34] Y. Jiang, J. B. Adams, and M. van Schilfgaarde, J. Chem. Phys. **123**, 064701 (2005).
[35] N. V. Skorodumova, S. I. Simak, B. I. Lundqvist, I. A. Abrikosov, and B. Johansson, Phys. Rev. Lett. **89**, 166601 (2002).
[36] C. Loschen, J. Carrasco, K. M. Neyman, and F. Illas, Phys. Rev. B **75**, 035115 (2007).
[37] J. L. F. Da Silva, M. V. Ganduglia-Pirovano, J. Sauer, V. Bayer, and G. Kresse, Phys. Rev. B **75**, 045121 (2007).
[38] N. V. Skorodumova, M. Baudin, and K. Hermansson, Phys. Rev. B **69**, 075401 (2004).
[39] T. Gürel and R. Eryiğit, Phys. Rev. B **74**, 014302 (2006).
[40] A. Rohrbach, J. Hafner, and G. Kresse, J. Phys.: Condens. Matter **15**, 979 (2003).
[41] M. Nolan, S. Grigoleit, D. C. Sayle, S. C. Parker, and G. W. Watson, Surf. Sci. **576**, 217 (2005).
[42] R. M. Martin, *Electronic Structure* (Cambridge University Press, Cambridge, England, 2004).
[43] P. E. Blöchl, Phys. Rev. B **50**, 17953 (1994).
[44] G. Kresse and D. Joubert, Phys. Rev. B **59**, 1758 (1999).
[45] G. Kresse and J. Hafner, Phys. Rev. B **47**, 558 (1993).
[46] G. Kresse and J. Furthmüller, Phys. Rev. B **54**, 11169 (1996).
[47] J. P. Perdew, K. Burke, and M. Ernzerhof, Phys. Rev. Lett. **77**, 3865 (1996).
[48] S. L. Dudarev, G. A. Botton, S. Y. Savrasov, C. J. Humphreys, and A. P. Sutton, Phys. Rev. B **57**, 1505 (1998).
[49] P. Vinet, J. Ferrante, J. H. Rose, and J. R. Smith, J. Geophys. Res. **92**, 9319 (1987).
[50] S. Özdemir Kart, M. Uludogan, I. Karaman, and T. Cagin, Phys. Status Solidi A **205**, 1026 (2008).
[51] K. Parlinski, Z-.Q. Li, and Y. Kawazoe, Phys. Rev. Lett. **78**, 4063 (1997).
[52] R. D. King-Smith and D. Vanderbilt, Phys. Rev. B **47**, 1651 (1993).
[53] J. L. F. Da Silva, Phys. Rev. B **76**, 193108 (2007).
[54] S. Fabris, G. Vicario, G. Balducci, S. deGironcoli, and S. Baroni, J. Phys. Chem. B **109**, 22860 (2005).
[55] F. Marabelli and P. Wachter, Phys. Rev. B **36**, 1238 (1987).
[56] E. Wuilloud, B. Delley, W. D. Schneider, and Y. Baer, Phys. Rev. Lett. **53**, 202 (1984).
[57] Z. Hu, R. Meier, C. Schüßler-Langeheine, E. Weschke, G. Kaindl, I. Felner, M. Merz, N. Nücker, S. Schuppler, and A. Erb, Phys. Rev. B **60**, 1460 (1999).